

Spatio-temporal correlations in human gamma band electrocorticograms

V. Menon^{a,b}, W.J. Freeman^{a,b,*}, B.A. Cutillo^a, J.E. Desmond^a, M.F. Ward^a, S.L. Bressler^a,
K.D. Laxer^c, N. Barbaro^c, A.S. Gevins^a

^a EEG Systems Laboratory, One Rincon Center, 101 Spear St. 204, San Francisco, CA 94105, USA¹

^b Division of Neurobiology, LSA 129, University of California, Berkeley, CA 94720, USA

^c Northern California Epilepsy Center, University of California, San Francisco, CA 94143, USA

Accepted for publication: 2 September 1995

Abstract

Animal electrocorticogram (ECoG) studies have shown that spatial patterns in the gamma band (> 20 Hz) reflect perceptual categorization. Spatio-temporal correlations were investigated in the 20–50 Hz range in search for similar phenomena in human ECoG. ECoGs were recorded in a somatosensory discrimination task from 64-electrode subdural grid arrays, with inter-electrode spacing of 1 cm, overlying somatosensory, motor and superior temporal cortices in 2 patients with intractable epilepsy. Bootstrap techniques were devised to analyze the spatial and temporal characteristics of the correlations.

Despite an extensive search, no evidence was found for globally correlated activity related to behavior either in narrow (i.e., 35–45 Hz) or broad (i.e., 20–50 Hz) bands. Spatial patterns, extracted using principal component analysis, could not be classified with respect to stimulus type in any time interval. Instead, spatially and temporally intermittent synchronization was observed between pairs of electrodes in 1 cm × 1 cm regions with high variability within and across trials. The distribution of correlation coefficients differed substantially from background levels at inter-electrode distances of 1 cm and 1.4 cm but not 2 cm or more. The minimum duration of correlation, the decorrelation time, of the ECoG was about 50 msec; the average correlation duration at 1 cm inter-electrode distance was about 150 msec; and the recurrence rate of significant correlation peaks was about 1.3/sec.

The findings suggest that the surface diameters of domains of spatially correlated activity underlying perceptual categorization in human gamma band ECoG are limited to less than 2 cm and that the intermittent synchronization observed across separations of 1 cm and 1.4 cm is not solely due to volume conduction. Thus, if such gamma band spatial patterns exist in the human brain, no existing technology would be capable of measuring them at the scalp, and subdural electrode arrays for cortical surface recording would have to have spacings under 5 mm.

Keywords: Human ECoG; Gamma; Spatio-temporal correlations; Bootstrap

1. Introduction

The existence of spatial patterns of neural activity in sensory cortices, corresponding to sensory stimuli, has been postulated for over a century, based on the anatomical discovery of topographic mappings of axonal thalamo-cortical projections onto the primary sensory cortices, and based on the subsequent physiological demonstrations of the mapping by the olfactory mucosa onto the bulb, of the complex log mapping by the retina onto the visual cortex,

of the tonotopic maps in the auditory cortex, and of the “homunculi” in the somatosensory cortex.

Microelectrode recordings of sensory evoked unit activity have led to the formulation of the “feature detector” hypothesis, according to which the spatial patterns of punctate activation of receptors are transformed into representations of primitives (odors, tones, moving spots, lines, etc.) in the discharges of single cortical neurons. This formulation has led to the still unsolved “binding problem” (Hardcastle, 1994), which concerns the mechanism by which the activity of a small collection of feature detectors might be coordinated into a spatial pattern, in order to represent each object that is behaviorally discriminated by the subject under recording.

* Corresponding author. Tel.: +1 510 6424220; E-mail: wfreeman@garnet.berkeley.edu.

¹ Address for reprint requests.

As an alternative to the feature hypothesis, it is proposed that sensory cortical neurons interact diffusely but densely to form a population, and that stimulus-evoked action potentials on afferent pathways serve to destabilize the population, leading to the emergence of a self-organized spatial pattern of activity as the cortical response to the stimulus (Freeman and Grajski, 1987). The contribution of any one or a few of the millions of neurons interacting to form the population is too small to be detected. Instead, it is necessary to record the local field potentials established by the flow of dendritic synaptic currents across the extra-neuronal tissue resistance.

A test of this hypothesis in the olfactory bulb was made by retrospective classification of multichannel ECoGs (Viana di Prisco and Freeman, 1985). Time segments of ECoGs were simultaneously recorded from electrodes with spacings of 0.5 mm in rabbits during presentations of odors that the subjects were trained to discriminate. Successful classification was achieved with respect to odors by extracting from each time segment of 64 traces a common wave form, and then regressing that wave form onto each trace to determine its local amplitude. The “perceptual code” turned out to be a spatial pattern of amplitude modulation (AM) of a common wave form, which was expressed by a 64×1 column vector giving a point in 64-space. Classification was done by a euclidean distance measure, which showed clustering of ECoG patterns in 64-space around a centroid for each discriminable stimulus (Freeman and Viana di Prisco, 1986; Freeman and Grajski, 1987).

The techniques have been successfully extended to the visual cortex of the monkey with 35 subdural electrodes at spacings of 5 mm (Freeman and Van Dijk, 1987), and to the visual, auditory, and somatic cortices of rabbits with 64 epidural electrodes at spacings of 0.6 mm (Freeman and Barrie, 1994). Further evidence of correlation of wave forms across multimillimetric distances has been reported from the cat visual cortex (Eckhorn et al., 1988; Gray et al., 1989), human auditory cortex by MEG (Llinás and Ribary, 1993), and primate sensorimotor cortex (Murthy and Fetz, 1992). Bullock et al. (1992) investigated coherence spectra of free running human ECoG using subdural strips of 8 electrodes 5–10 mm apart. They found that coherence fell to 0.5 over distances of 5–10 mm for all frequencies. Intermittent synchronization in the gamma range has also been reported between widely separated transcortical electrodes in the striate, prestriate, inferotemporal, motor and frontal cortices of the monkey (Bressler et al., 1993).

The present report describes an attempt at replication of the animal studies in 2 neurosurgical patients, each having a grid of 64 subdural electrodes with spacings of 10 mm placed over the fronto-temporo-parietal area. Our results from cross-correlations of brief segments of multiple ECoGs indicate that the electrodes were too far apart to reveal the commonality of wave form that was the basis

for amplitude modulation spatial pattern classification in animals. Spatially and temporally intermittent synchronization above the level of noise and background fluctuations was observed across inter-electrode separations under 2 cm. (In this report, synchronization is used to imply the existence of peaks in real-time zero-lag correlation.) The analyses suggest that the average diameter of cortical populations, forming a mosaic (Calvin, 1994) of interactive patches, and providing the substrate for human perception and cognition, may be under 2 cm, requiring an electrode spacing of less than 5 mm for adequate spatial sampling.

A brief summary of these results has been presented at the annual meeting of the Society for Neuroscience (Menon et al., 1994).

2. Methods and materials

2.1. Subjects

Two right-handed female patients aged 37 (no. 1) and 19 years (no. 2), undergoing neurosurgery for control of medically refractory complex partial seizures at the Northern California Epilepsy Center of the University of California at San Francisco, volunteered to participate in the study, and were familiarized with the experiment.

2.2. Experiment

Details of the experiment are described elsewhere (Gevins et al., 1994, 1995). Briefly, on each trial the subjects received 1 of 3 electrical stimuli to the little finger on the hand contralateral to the grid. Pulses were generated by a Grass S-11 dual output stimulator, with pulse durations of 20, 60 and 500 μ sec, perceived respectively as low, medium and high intensity. Flexion responses of force 0.2 and 0.8 kg respectively were to be made to the low and medium intensity stimuli with the index finger on the same hand on a Grass FT-03 displacement transducer. Response was to be withheld to high intensity stimuli. Stimuli were presented 1 sec after a visual cue. Visual feedback was presented indicating whether the response was correct, with the exact pressure and error in the case of response trials, at 500 msec after response completion. On no-response trials, the feedback appeared 1.7 sec after the stimulus. The next successive trial began 4 sec after the onset of feedback.

2.3. Recordings

Cortical EEG (ECoG) was recorded with 64-electrode (8×8) subdural grid arrays. Stainless steel electrodes measuring 5 mm in diameter were embedded in a rectangular array in a transparent silastic sheath with 10 mm center to center inter-electrode distance. For both patients,

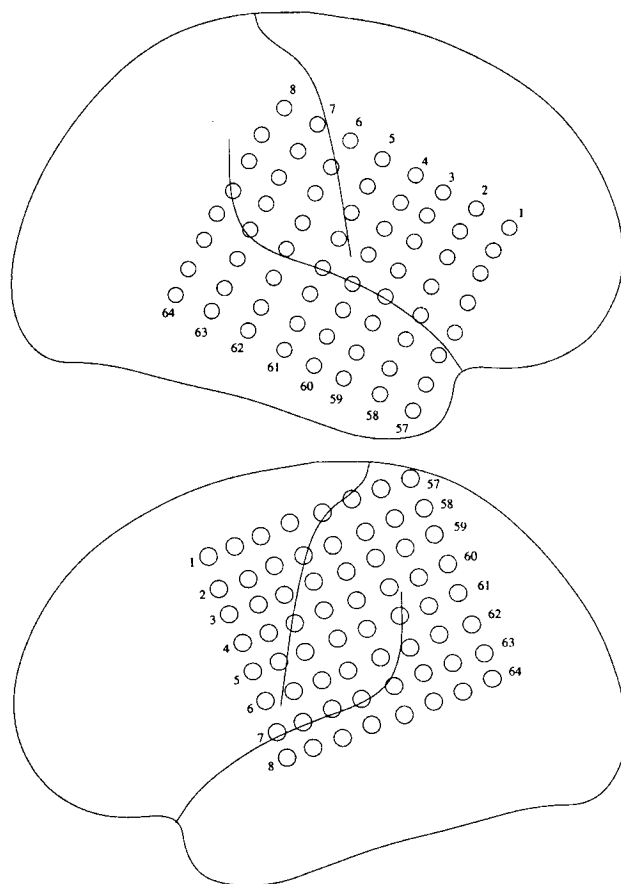


Fig. 1. Locations of 64-electrode subdural grids over somatosensory, motor, and temporal cortices are shown with respect to central and lateral sulci. Top: right hemisphere of patient no. 1. Bottom: left hemisphere of patient no. 2. Inter-electrode distance was 1 cm and electrode size was 0.5 cm.

ECoG was recorded referenced to skull screws near Cz. EMG to finger flexion was also recorded with bipolar electrodes over the flexor digitoris. Stimulation studies were performed for clinical functional localization using monopolar recordings. Details of the methods used to register the grid with cortical areas are described by Gevins et al. (1994).

For patient no. 1, the grid overlay somatosensory, motor and temporal cortices in the right hemisphere centered on the sylvian fissure and central sulcus (Fig. 1A). Additionally, a 6-contact depth electrode was placed in the middle temporal gyrus directed medially, having the most distal contact at the amygdala, and the most lateral one at the middle temporal gyrus between grid electrodes 59 and 60. Five depth electrodes were used in place of grid electrodes 4–8. ECoG was amplified (gain 5000), bandpass filtered (0.5–100 Hz, –3 dB at 100 Hz, 36 dB/octave roll-off) and sampled at 210 Hz. For patient no. 2, the grid overlay somatosensory, motor and superior temporal cortices in the left hemisphere (Fig. 1B). Electrodes 56 and 62–64 were not used. ECoG was amplified (gain 5000), bandpass filtered (0.5–80 Hz, –3 dB at 80 Hz, 18 dB/octave

roll-off) and sampled at 240 Hz. Sampled data for both patients were stored on high-quality VHS video tape at the Epilepsy Center in UCSF. The analog video tape signal was later decoded at EEG Systems Laboratory, sampled at 256 Hz, 16 bits/sample, and transferred to hard disk along with stimulus and event-timing information about each trial.

About 600 trials were collected from each patient in blocks of 20 trials. Each recording segment lasted 4.5 sec, starting from 1.6 sec preceding the stimulus to 1.3 sec following the feedback onset.

2.4. Analysis

Each trial was edited manually for artifacts. Trials with instrumental artifacts, seizure or other abnormal activity were eliminated. Response trials with reaction times greater than 1 sec were eliminated; the remaining trials were classified as correct or incorrect on the basis of the distributions of actual pressure applied. In patient no. 1, electrodes 1, 2, 3, 26, 58, 63 and 64 were eliminated from further consideration due to instrumental problems or inadequate number of artifact-free trials (fewer than 20), leaving a total of 52 electrodes for analysis. Similarly, in patient no. 2, electrodes 56–61 were eliminated leaving a total of 54 electrodes for analysis.

To independently assess the extent of localization of changes in ECoG related to stimulus and response, evoked potentials and changes in power spectral density (PSD) were investigated. Evoked potentials were computed by averaging artifact-free trials. The width at half maximum (WHM) for each EP peak was defined as the inter-electrode distance across which the potential was greater than half the maximum.

PSD was computed on unfiltered data using a Welch window to minimize leakage (Press et al., 1992). Average PSDs in the mu (7–14 Hz), beta (14–20 Hz), and gamma (20–50 Hz) bands were computed. Changes in the average PSD associated with stimulus and response were sought in 3 time intervals: 1 pre stimulus (–500–0 msec) and 2 post stimulus (0–500 msec and 500–1000 msec). Student's paired *t* test was used to assess the significance of changes in average PSDs between the –500–0 msec and 0–500 msec intervals and between the 0–500 msec and 500–1000 msec intervals. In addition, Student's *t* test was used to compare changes in average PSD between conditions in each of the 3 intervals.

2.5. Spatio-temporal correlations

The time series were bandpass filtered in the 20–50 Hz range (Hamming filter, 6 dB down at 20 Hz and 50 Hz). A moving window 100–300 msec long was stepped every 4 msec for temporal segmentation of the 52–54 simultaneous traces. Correlation coefficients were computed in real

time without lag using segments from pairs of electrodes. Principal components analysis (PCA) (Hays, 1994) was performed using 100–300 msec temporal segments from sub-arrays of 9 electrodes using electrodes as the independent variable. The eigenvalues of the correlation matrix defined the fraction of variance explained by each component. The principal components themselves defined spatial patterns representing the commonality of the wave forms. Non-parametric discriminant analysis (k-nearest-neighbor method) was used to test classification of spatial patterns between stimulus types (Gevins et al., 1979; Gevins, 1980; Freeman, 1987).

Even random signals generate spurious correlations as a result of filtering. Therefore, the characteristics of spatio-temporal correlations were analyzed in greater detail by bootstrap methods (Gevins et al., 1989; Efron and Tibshirani, 1993). In the variant of the bootstrap method used here, expected probability distributions for the spatio-temporal correlations were derived and the measured ECoG correlations were compared to these distributions to assess their significance at various inter-electrode distances.

Two different types of distribution were computed. The first distribution was computed from 2 independent filtered random time series. The time series were generated with a

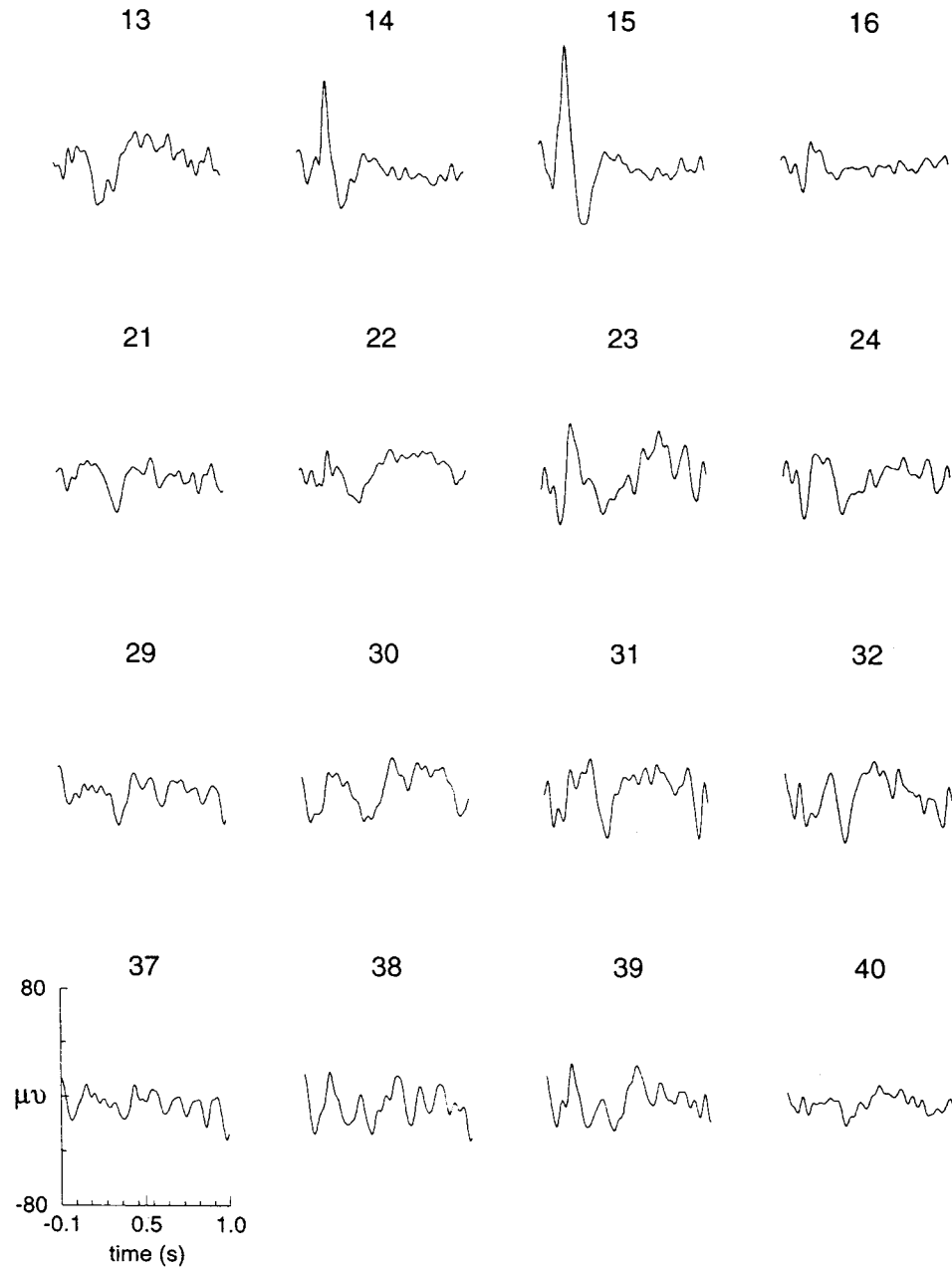


Fig. 2. Stimulus locked averaged evoked potentials (EPs) to high intensity stimuli recorded from electrodes overlying the somatosensory (14–16, 22–24 and 29–32), motor (13 and 21) and superior temporal (37–40) cortices in patient no. 1. The largest EPs were recorded at electrodes 14 and 15. The half width of each peak, defined as the distance at which the peak reduced to half its maximum value, was less than 1.4 cm.

gaussian distribution, zero mean and unit standard deviation (Press et al., 1992). Correlation coefficients were computed using the same segmentation and filtering schemes used for ECoGs. The distribution of correlation coefficients obtained in this manner defined the noise distribution.

A second type of distribution was computed incorporating systematic biases in the data, including those arising from short range temporal correlation in the ECoG. To define this distribution, a threshold inter-electrode distance, defined as the distance beyond which the distribution of correlation coefficients did not change significantly, was first computed. The distribution of correlation coefficients computed at this threshold inter-electrode distance defined the background distribution.

Distributions of correlation coefficients were compared using the Kolmogorov-Smirnov (KS) test. A Bonferroni correction (Hays, 1994) was applied in order to take into account the effect of temporally dependent segments. The correction factor was taken to be the number of non-overlapping temporal segments in the simultaneous time series. For example, for distributions of correlation coefficients derived using 1.1 sec post-stimulus intervals from 64 trials

with 100 msec windows shifted every 4 msec, the number of observations was 16,000. However, the number of independent observations equals 640. To assess significance at the $P < 0.005$ level, a Bonferroni corrected P value of $0.005/640$ was used.

The minimum duration of correlation was computed using the decorrelation time of the ECoG. The decorrelation time is the time beyond which the ECoG (at a single electrode) is not correlated with itself. The decorrelation time was determined using the auto-correlation function. For aperiodic time series, the first zero crossing of the auto-correlation determines the decorrelation time.

To estimate an upper limit on the duration of correlation, the effect of window size on the magnitude of the correlation coefficients was examined. As the window size was increased, peaks in correlation broadened but reduced in magnitude. The reduction of the number of peaks to that of the noise and background distributions was used to estimate an upper bound to the duration of the correlation segment. Critical values for $P = 0.01$ were determined from both noise and background correlation coefficient distributions. The critical value was the $P \times N$ th value in the rank ordered list of correlation coefficients, where N

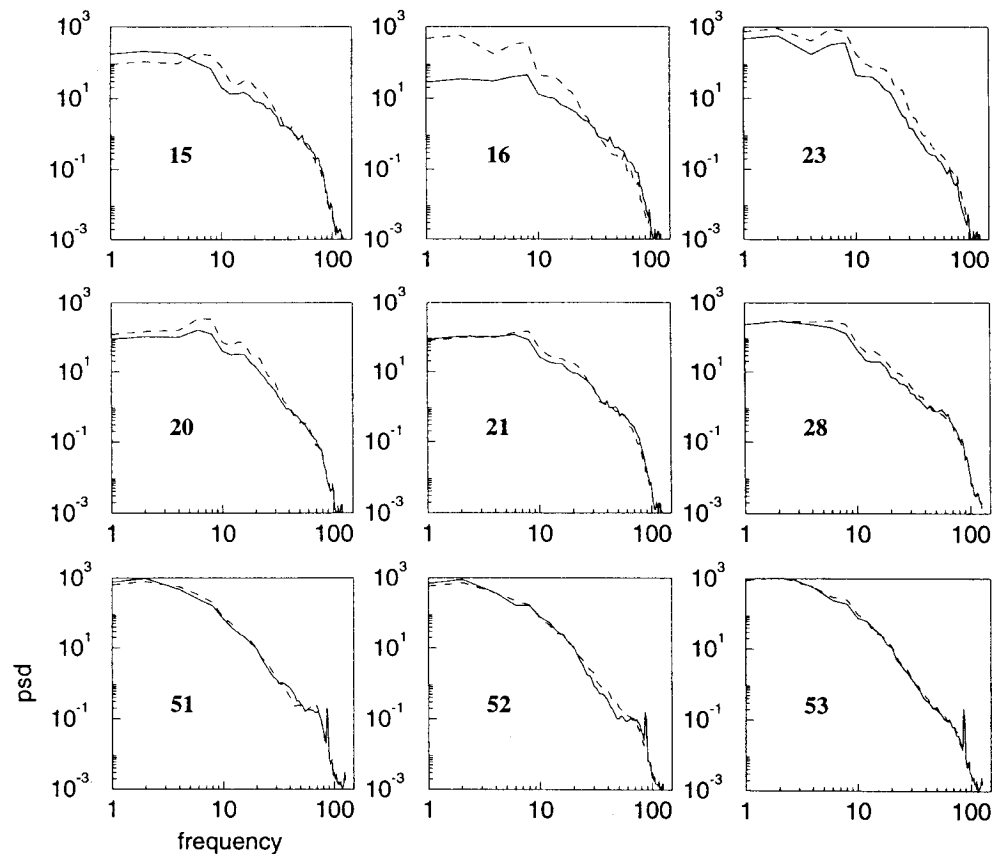


Fig. 3. Power spectral density (PSD) of 500 msec post-stimulus (solid line) and 500 msec pre-stimulus (dotted line) ECoG segments from patient no. 1. PSD in the somatosensory cortex (electrodes 15, 16 and 23), motor cortex (electrodes 20, 21 and 28) and temporal cortex (electrodes 51–53) indicated aperiodic $1/f$ activity in the mu, beta and gamma bands. PSD was computed by averaging spectra across 78 high stimulus intensity trials. All graphs are in log-log scale with PSD in $\mu V^2/Hz$.

was the number of correlation coefficients. The number of peaks with correlations above the critical value was then analyzed as a function of window size.

3. Results

3.1. Clinical observations

In patient no. 1, stimulation of electrode 7 produced thumb and finger flexion, stimulation of electrode 8 produced tingling sensations in fingers and stimulation of electrode 20 inhibited movement of the left hand. Seizure events were observed originating in the temporal depth electrode (placed between grid electrodes 59 and 60) which propagated dorsally. In this active region, complex partial seizure activity was maximal in electrodes 60–63 and 52–53. Following the experiment described here, a region consisting of the anterior temporal lobe measuring 6 cm at the superior temporal gyrus, 7.5 cm at the inferior temporal gyrus, and including the amygdala and 2 cm of the hippocampus, was resected. As a result, the patient recovered normally and has since been seizure free.

In patient no. 2, stimulation of electrodes 35 and 36 produced extension of the little finger and stimulation of electrode 43 produced numbness in fingers 3–5. The post-experiment resection in this patient consisted of a small topectomy in the superior parietal lobule. However, since the patient continued to suffer from seizures, the presence of a frontal seizure focus was suspected.

3.2. Behavioral observations

Of 600 trials presented, 436 were performed correctly by patient no. 1. The fraction of correct responses was 87%, 62% and 57% for high, low and medium intensity stimulus trials respectively. Mean reaction times for correct responses were 813 ± 12 msec and 835 ± 11 msec for low and medium intensity stimuli respectively. Of 700 trials presented, 425 were performed correctly by patient no. 2 with accuracy rates of 83%, 52% and 50% for high, low and medium intensity stimuli respectively. Mean reaction times were 725 ± 12 msec and 745 ± 12 msec for low and medium intensity stimuli respectively. Both patients reported particular difficulty in recognizing medium intensity stimuli.

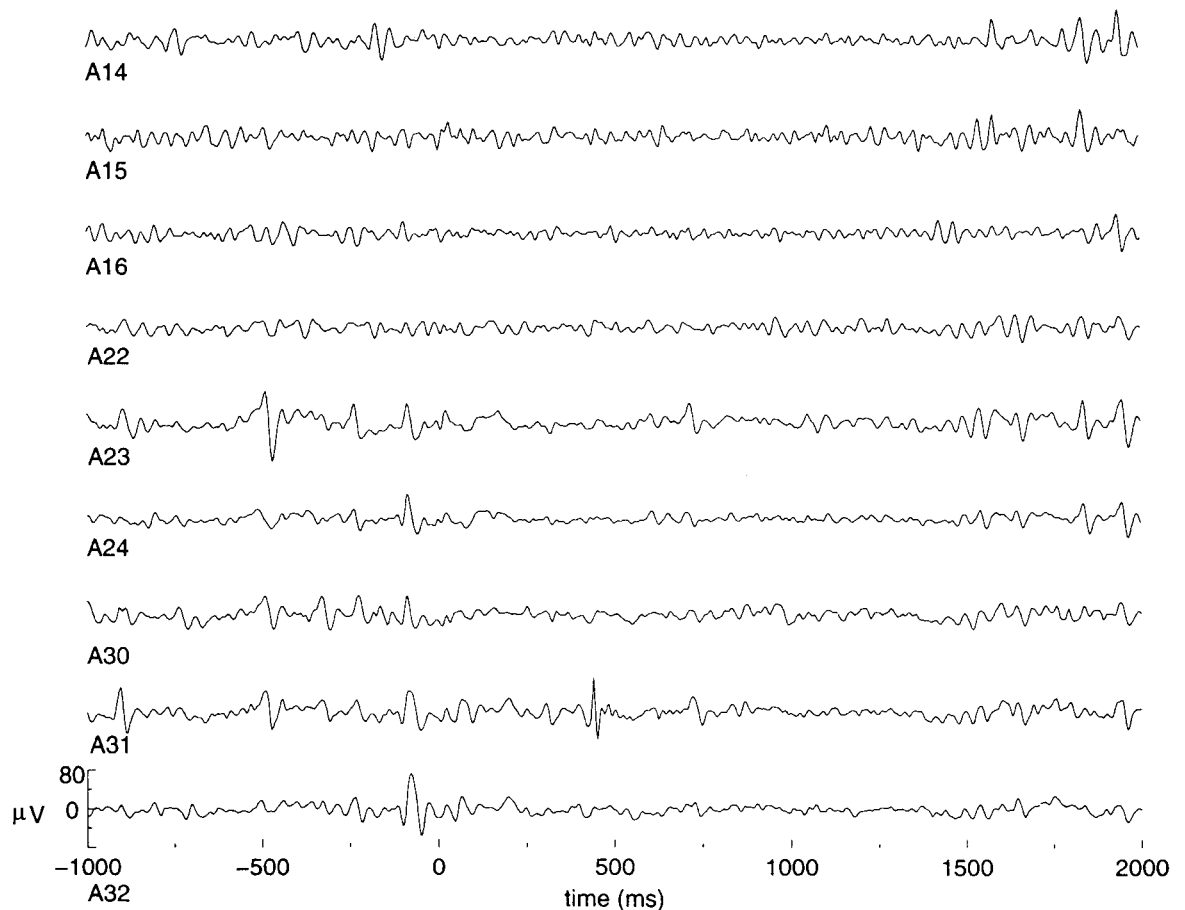


Fig. 4. Gamma band (20–50 Hz) filtered ECoGs from 9 electrodes in the post-central gyrus. One second pre-stimulus and 2 sec post-stimulus segments from a high stimulus intensity trial are shown. Inspection of these and other such traces indicates lack of sustained commonality of wave forms even between nearest-neighbor electrodes.

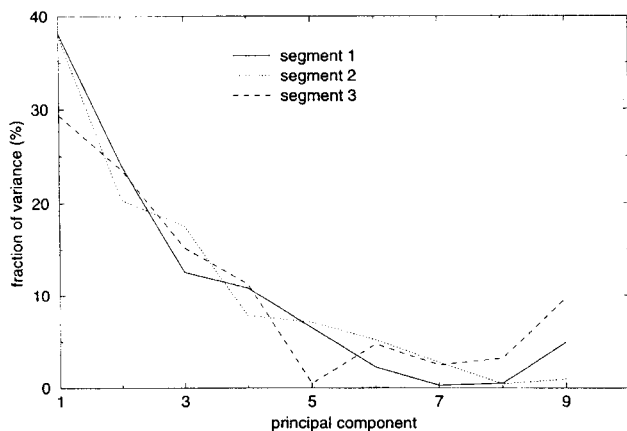


Fig. 5. The fraction of variance explained by the principal components in a principal components analysis (PCA) of three 200 msec segments from the 9 electrodes shown in Fig. 4. Segment 1 spanned a 200 msec pre-stimulus interval (–200–0 msec), segment 2 spanned the 0–200 msec post-stimulus interval, and segment 3 spanned the 200–400 msec post-stimulus interval. In each of these segments, 5–7 components were needed to explain 90% of the variance. By comparison, in 5 mm × 5 mm 64-electrode arrays used in animal studies, the first component sufficed to explain 80–95% of the variance. This is indicative of the lack of commonality of the human gamma band ECoG wave forms at separations of 1–2 cm.

3.3. Evoked potentials

Stimulus evoked potentials (EPs) were computed by averaging 100 behaviorally correct artifact-free trials. In

patient no. 1, the largest EPs were recorded at electrodes 14 and 15 (Fig. 2). The P100 and N140 components were localized to electrodes 14 and 15. The WHM of each of these peaks was less than 1.4 cm. In the case of patient no. 2, the largest EPs were recorded at electrodes 27, 34, 35, 36 and 43. The P30 and N350 components were largest at electrode 36. The N140 was largest at electrode 27. The WHM of each of these peaks was less than 2 cm.

3.4. Spectra changes with stimulus and response

PSD estimates obtained by averaging spectra of 500 msec pre- and post-stimulus segments across no-response (high stimulus intensity) trials showed a nearly linear relation between log frequency and log power (“1/f”) in the mu, beta and gamma bands (Fig. 3). In the interval immediately following stimulus onset, the average PSD decreased in all 3 frequency bands. This decrease was observed at several electrodes in the sensorimotor cortex and a few electrodes in the pre-motor cortex on both response and no-response trials. Comparison of the mean PSDs in the pre- and the first 500 msec post-stimulus intervals across 78 trials revealed that the decrease was statistically significant (paired *t* test, $P < 0.005$, *df* (77)). In patient no. 1, the decrease was observed in electrodes 14–16, 20, 23–24 and 30–32. In patient no. 2, a statistically significant decrease (paired *t* test, $P < 0.005$, *df* (77)) was observed in electrodes 19, 21, 25–27, 34–35 and 37–39.

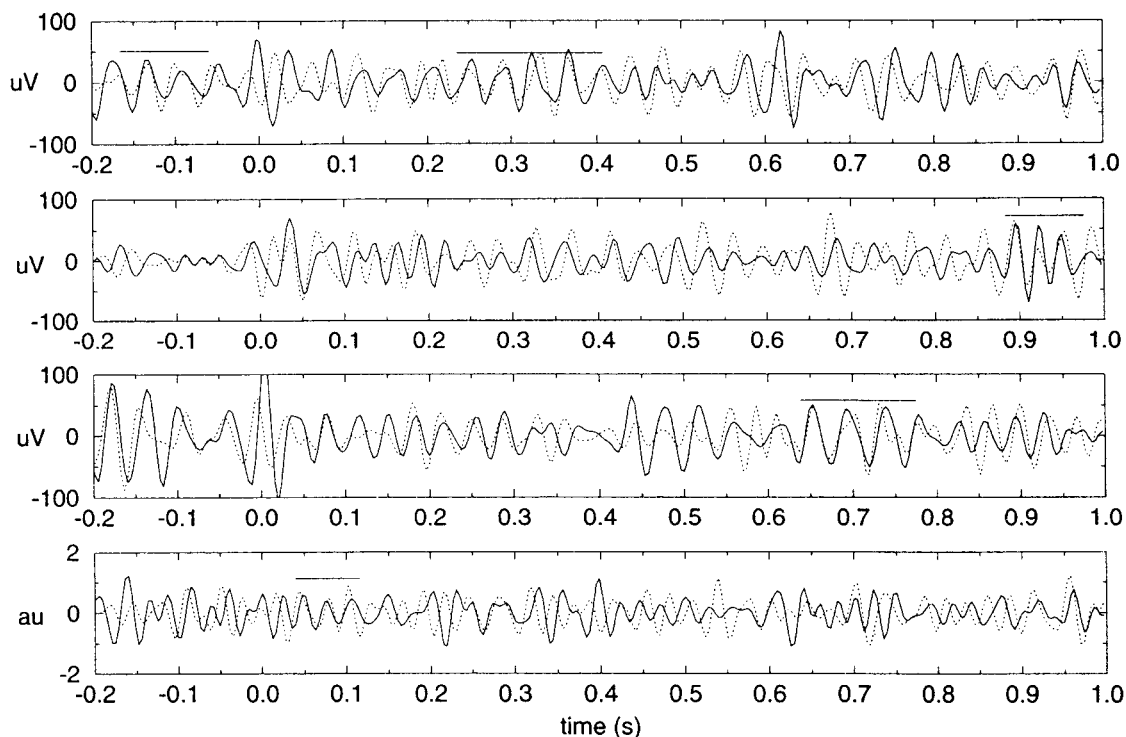


Fig. 6. Intermittent synchronization of gamma band ECoGs was observed in both pre-stimulus (–0.2–0 sec) and post-stimulus (0–1 sec) intervals. The upper 3 graphs show filtered (20–50 Hz) ECoG from 3 different high stimulus intensity trials. ECoG from electrodes 14 and 15 (solid and dotted lines respectively), where the largest stimulus evoked potentials were recorded, are shown. For comparison, the bottom graph illustrates intermittent synchronization in 2 filtered random time series (arbitrary units, au).

On these same electrodes, response trials differed from these no-response trials only in the second post-stimulus interval (t test, $P < 0.001$, df (154)). This interval overlapped the mean response time. The difference was caused partly by increase in PSD for no-response trials and partly by decrease in PSD for response trials in the second post-stimulus interval (in comparison with the first post-stimulus interval). No spectral differences were detected in the temporal cortex of either patient, except for an occasional electrode near the lateral sulcus.

3.5. EEG time series – lack of commonality

Fig. 4 shows gamma band filtered pre- and post-stimulus ECoG segments from electrodes in the post-central gyrus in patient no. 1. Visual inspection of these and other traces indicates lack of sustained commonality of wave forms even between nearest-neighbor electrodes. ECoG segments from patient no. 2 also indicated a lack of commonality of the wave forms.

Principal component analysis was performed on the correlation matrix obtained from 200 msec gamma band filtered segments drawn from sub-arrays of 9 electrodes. Five to 7 principal components were needed to incorporate a variance of 90% (Fig. 5). The dominant component accounted for only 30–40% of the variance. Discriminant

analysis did not reveal any differences between high, low or medium intensity trials. Classification rates were typically at the chance level for all 200 msec segments between 1 sec pre stimulus to 1 sec post stimulus.

3.6. Spatial and temporal intermittency

Inspection of selected pairs of electrodes revealed that the level of correlation varied considerably with time across a trial. Intermittent correlated activity was observed between pairs of electrodes (Fig. 6). Comparison of the same electrode pair across trials indicated high and unpredictable variability unrelated to behavior. Examples of variability across trials are shown in Fig. 7A using data from electrodes 14 and 15 in patient no. 1 where the largest EPs were recorded. Averaging the Fisher Z-transformed correlation coefficients across 64 trials as a function of time did not reveal any time interval with reproducibly high correlations (Fig. 7B). Mean correlation across all trials and intervals was 0.35. For patient no. 2, the mean correlation across all trials and intervals between electrodes 36 and 35, where the largest EPs were recorded, was 0.20; the largest mean correlation recorded was 0.43, between electrodes 28 and 29. Similar results were found for all other electrode pairs for both patients.

To investigate the extent of spatial commonality, a 1

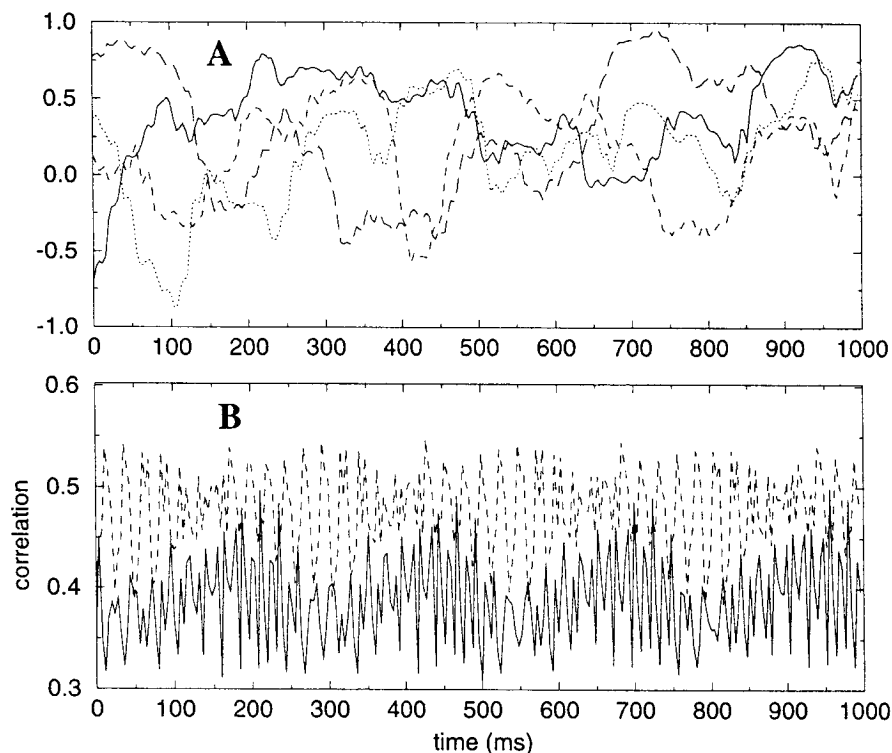


Fig. 7. Variability in gamma band correlations between nearest-neighbor electrodes (1 cm inter-electrode distance) with time and across trials. Correlations between electrodes 14 and 15 (patient no. 1), where the largest stimulus evoked potentials were recorded, are shown. A: variation of correlation with time across 4 sample trials. B: mean (solid line) and standard deviation (dashed line) of correlations across 64 trials. The mean and standard deviation were computed from Fisher Z scores and then transformed back to correlation coefficients. Similar variability was found for other electrode pairs in both patients. Correlations were computed with 100 msec windows incremented every 4 msec. The ECoG was bandpass filtered (20–50 Hz).

cm \times 1 cm area of the cortical surface, where the largest EPs were recorded (electrodes 14, 15, 22 and 23 in patient no. 1), was selected. On repeated trials, traces from single electrodes paired with simultaneously recorded traces from nearest-neighbor and second nearest-neighbor electrodes often showed high negative and positive correlations in the same segments, and the levels changed intermittently and unpredictably (Fig. 8A). However, this temporally intermittent synchronization did not extend beyond the second nearest neighbor (inter-electrode separation of 2 cm) or beyond (Fig. 8B).

Similar results were obtained for ECoGs from patient no. 2. Fig. 9A shows the pairwise correlations in a 1 cm \times 1 cm area where the largest stimulus evoked potentials were recorded in patient no. 2, electrodes 28, 29, 36 and 37. Intermittent synchronization was evident in these electrodes, but did not extend to the neighboring electrodes (Fig. 9B). Visual inspection of all single trials revealed no consistent changes arising from stimulus onset. No “phase resetting” was seen on any consistent basis and no differences were found between response and no-response trials. Similar results were obtained with ECoGs filtered in other frequency ranges around “40 Hz” (for example, bandpass 35–45 Hz, Hamming filter, -6 dB at 35 and 45 Hz).

3.7. Variation of spatio-temporal correlations with inter-electrode distance

For each stimulus type, distributions of correlation coefficients were derived with 1.1 sec post-stimulus intervals from 64 trials using 100 msec windows shifted every 4 msec. One hundred and fifty-three pairs of inter-electrode correlations in patient no. 1 and 406 pairs in patient no. 2 were examined for inter-electrode separations up to 5 cm. For all electrode pairs, distributions of correlations did not differ between pre- and post-stimulus segments (KS test, $P > 0.1$). The distributions of correlations between stimulus types also did not differ (KS test, $P > 0.1$). The distributions at inter-electrode distances of 1 cm and 1.4 cm were almost always significantly different from the distributions at inter-electrode distances of 2 cm or more (KS test, $P < 0.005$). Beyond 2 cm there was, in general, no dependence on distance. This defined a threshold distance of about 2 cm. Distributions obtained from electrode pairs at separations greater than this threshold distance were therefore used as estimators of the background distribution. The background distribution was statistically different from the noise distribution (KS test, $P < 0.005$).

As an additional measure of the degree and extent to

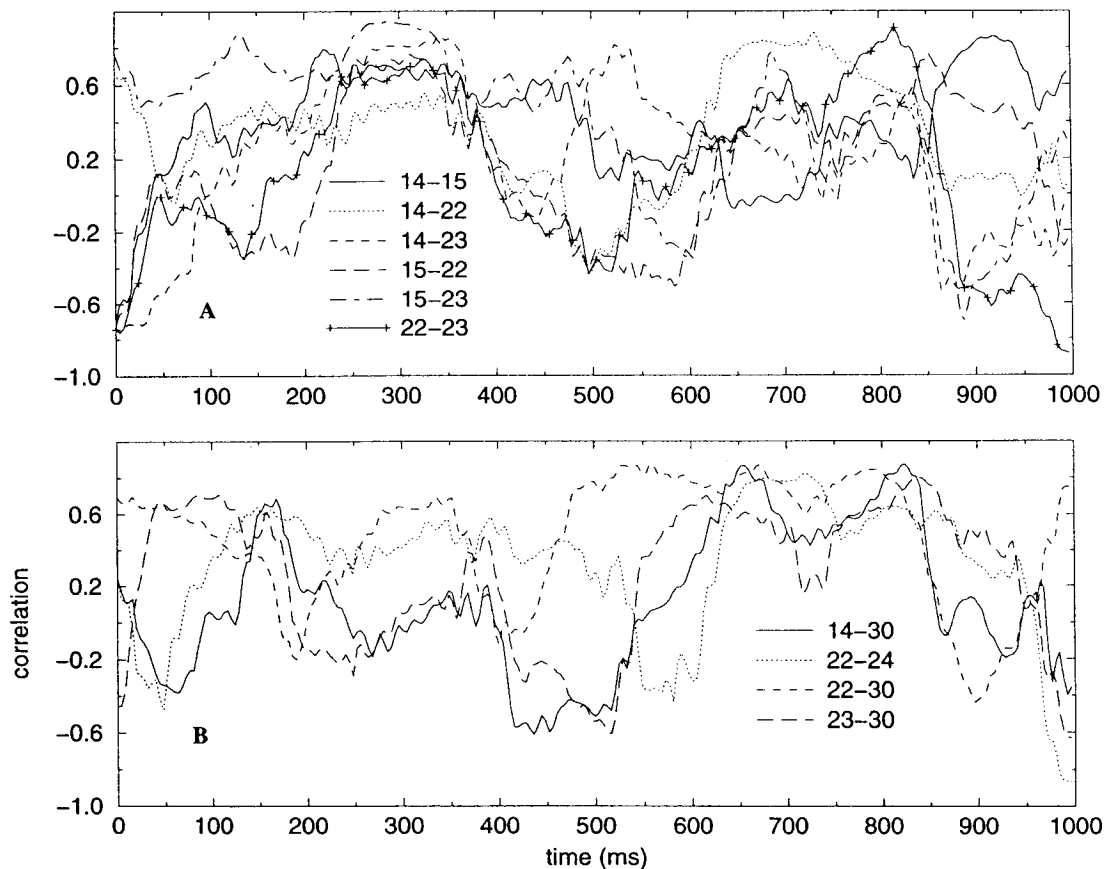


Fig. 8. Spatially localized intermittent gamma band synchronization in a 1 cm \times 1 cm region in the somatosensory cortex of patient no. 1. Top: pairwise correlations between electrodes 14, 15, 22 and 23 in patient no. 1 where the largest stimulus evoked potentials were recorded. Nearest and next-to-nearest neighbors show differing degrees of correlation with brief periods of intermittent synchronization. Bottom: pairwise correlation between electrodes in the surrounding region suggests lack of global synchronization. Correlations were computed using a 100 msec window on bandpass filtered (20–50 Hz) ECoG.

which the spatio-temporal correlations varied with inter-electrode distance, the skewness of distributions was examined. For each inter-electrode separation, the skewness estimates of distributions obtained from 4–6 pairs of electrodes were averaged. At inter-electrode separations of 1 cm, within either the post- or pre-central gyri, the distributions had a skewness of -0.60 , compared with -0.03 for the filtered noise distribution (Fig. 10A). The skewness of the distributions reduced to noise levels at separations of about 2 cm or more as indicated by the rapid drop in the negative skewness in both patient no. 1 (Fig. 10B) and patient no. 2 (Fig. 10C). Between gyri, the skewness of the distributions dropped to that of noise distributions at inter-electrode separations of 1.4 cm or more.

3.8. Duration of correlation segment

Using 1 sec post-stimulus segments, the minimum duration of correlation, determined from the decorrelation time of the auto-correlation function, was found to be 50–75 msec for ECoGs from both patients. The noise time series,

on the other hand, decorrelated within 1 time unit (about 4 msec).

The number of significant peaks (above a specified threshold) was computed using windows of 100, 150, 200, 250, 300, 400 and 500 msec duration. Windows smaller than the decorrelation time (50–75 msec) were not used. At a significance level of $P = 0.01$, the critical value of the frequency of peaks was about 0.85/sec for the background distribution and 0.75/sec for the noise distribution. At these critical values, the expected number of significant peaks/sec was about 0.45/sec for background distributions and 0.39/sec for noise distributions. The frequency of peaks generally fell to the expected background levels for windows of 175–250 msec and to noise levels at 300–375 msec (Fig. 11). For the example shown in Fig. 11, nearest-neighbor electrodes 15 and 23 (patient no. 1) and electrodes 28 and 29 (patient no. 2) were used. The largest evoked potentials were recorded at these electrodes. Both noise and background distributions were estimated using 100 msec windows. The background distribution for patient no. 1, estimated using ECoGs from electrodes 16

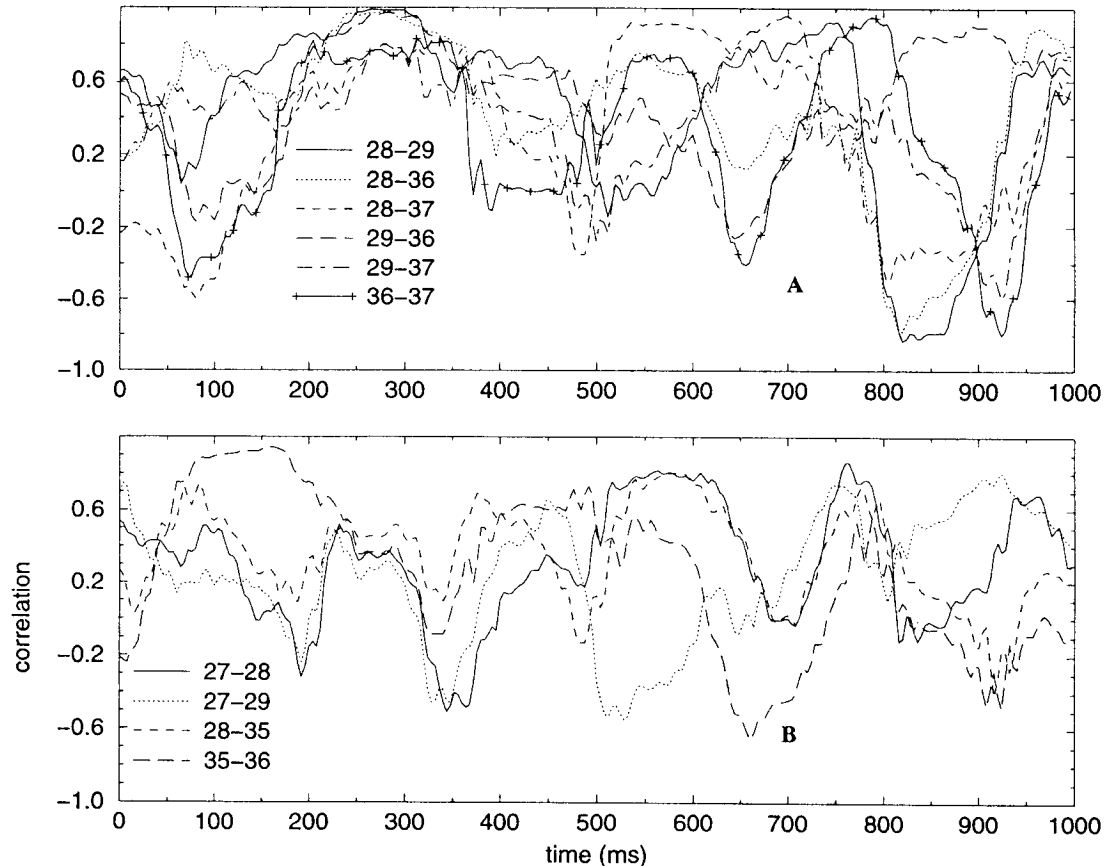


Fig. 9. Spatially localized intermittent gamma band synchronization in a 1 cm \times 1 cm region in the somatosensory cortex of patient no. 2. Top: pairwise correlations between electrodes 28, 36, 29 and 37 in patient no. 2 where the largest stimulus evoked potentials were recorded. Nearest and next-to-nearest neighbors show differing degrees of correlation with brief periods of intermittent synchronization. Bottom: pairwise correlation between electrodes in the surrounding region indicates lack of global synchronization. Correlations were computed using a 100 msec window on bandpass filtered (20–50 Hz) ECoG.

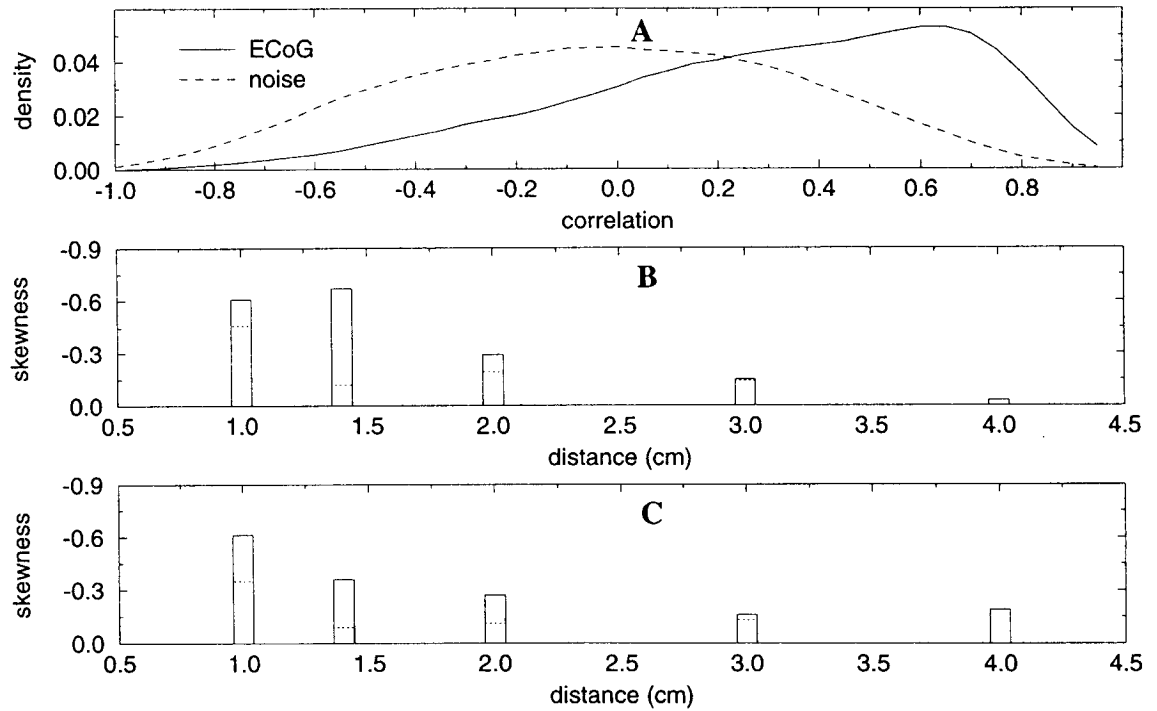


Fig. 10. The distribution of gamma band correlation coefficients reduced to noise levels at distances of 2 cm or more as indicated by the rapid drop in the negative skewness. A: asymmetric distribution of correlation coefficients obtained from electrodes separated by 1 cm (electrodes 14 and 15, patient no. 1) has a skewness of -0.6 which differed significantly from the symmetric distribution obtained from filtered noise. B: decrease in skewness of the distribution of correlation coefficients as a function of inter-electrode distance in patient no. 1. Results based on 18 electrode pairs within gyri (solid bar) and across gyri (dashed line). C: decrease in skewness as a function of inter-electrode distance in patient no. 2. Results based on 29 electrode pairs. Correlations were computed using 100 msec windows incremented every 4 msec on 1–1.5 sec post-stimulus ECoG from 64 high stimulus intensity trials. ECoGs and noise were both bandpass filtered (20–50 Hz).

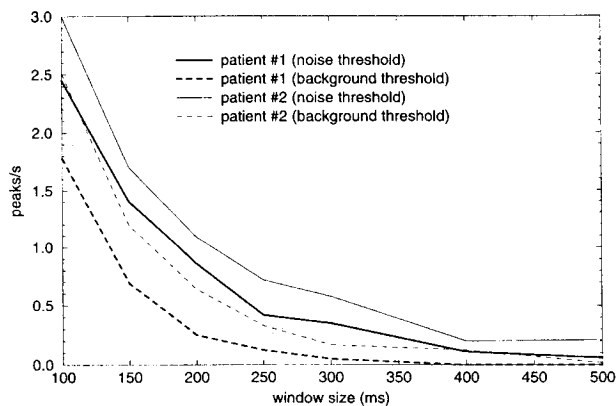


Fig. 11. Effect of window size on the number of significant peaks in gamma band correlation coefficients computed across electrodes separated by 1 cm. The number of significant peaks was assessed with noise and background thresholds. The number of peaks reduced to expected background levels at 175–250 msec and to expected noise levels at 300–375 msec. Expected values for the background and noise levels were 0.45/sec and 0.39/sec respectively. Peaks above a threshold of 0.78 were considered significant at $P < 0.01$ for comparison with noise levels. Peaks above a threshold of 0.85 (patient no. 1) and 0.83 (patient no. 2) were considered significant for comparison with background levels. Results shown above are for ECoG from electrodes 15 and 23 in patient no. 1 and electrodes 28 and 29 in patient no. 2. One to 1.5 sec post-stimulus segments from 64 high stimulus intensity trials were used. The ECoG was bandpass filtered (20–50 Hz).

and 29 (inter-electrode distance 4.2 cm), had a threshold value of 0.85/sec. The background distribution for patient no. 2, estimated using ECoGs from electrodes 35 and 38 (inter-electrode distance 3 cm), had a threshold value of 0.83/sec. The noise threshold at the $P = 0.01$ level was estimated to be 0.78/sec.

These observations suggest that the duration of correlation ranged from 50 to 250 msec. From the mean duration of correlation the approximate recurrence rate of the peaks was evaluated using the individual background distributions. Assuming a mean duration of 150 msec, the recurrence rate was about 1.3 peaks/sec. In both patients, similar results were found for other electrode pairs within the post- and pre-central gyri.

4. Discussion

The aperiodic but non-random nature of the gamma band ECoG was evident from the spectra (Fig. 3) and auto-correlation functions. Although bursts in the range 25–35 Hz have been reported in depth recordings in the sensorimotor cortex of monkeys (Murthy and Fetz, 1992; Sanes and Donoghue, 1993), no consistent evidence for this was found in the present human study. Contrary to

some recent reports, based on extracranial magnetoencephalograms (Llinás and Ribary, 1993), no peaks were observed at 40 Hz. The “ $1/f$ ” form of the spectra conformed to similar findings for the neocortex of the monkey (Freeman and Van Dijk, 1987; Bressler et al., 1993) and rabbit (Freeman and Barrie, 1994). In all cases, conjoint changes in PSD across the mu, beta, and gamma spectral domains suggested that neural events manifested in the ECoG were the product of broad spectrum, chaotic dynamics of neural populations (Freeman, 1991), and did not manifest narrow band resonance phenomena at particular frequencies such as “40 Hz.”

Task-related spectral modulation of gamma band ECoG was observed across several electrodes in the somatosensory and motor cortices, and a few electrodes in the pre-motor cortex. No spectral modulation was detected in any of the electrodes overlying the temporal cortex. The results confirm previous findings of spatially localized desynchronization of the mu, beta and gamma bands of the human ECoG due to movement (Arroyo et al., 1993). The desynchronization in the gamma band is also in agreement with blocking of local field potential oscillations in the 15–50 Hz range reported in primate motor and pre-motor cortices (Sanes and Donoghue, 1993). No evidence was found for gamma band task-related synchronization (Pfurtscheller and Neuper, 1988). These results are in contrast with conventional low frequency evoked potentials, in which highly significant differences were found between the same experimental tasks (Gevins et al., 1996).

Visual inspection revealed no “phase resetting” (Llinás and Ribary, 1993) in any frequency range nor did segments of high correlation last long enough to allow definition of such events. No consistent phase shifts across electrodes were observed in the gamma band. Principal component analysis indicated that 5–7 components were needed to account for 90% of the variance. In comparison, previous animal studies on 5 mm \times 5 mm sub-dural arrays indicated a substantially higher degree of spatial commonality in the ECoG wave forms. A single component sufficed to explain 80–98% of the variance in the animal studies. Further, unlike the animal studies, spatial patterns derived from the principal components of human gamma band ECoG could not be classified with respect to the different stimulus types in any time interval.

No task-related differences were found in the extent or degree of spatial correlation, which was spatially and temporally intermittent, and characteristically insignificant across distances exceeding 2 cm. Levels of gamma band spatial correlation were unrelated to the stimuli and responses. Three-way pairs of nearest-neighbor and second nearest-neighbor electrodes could show drastically differing levels of correlation simultaneously. Pairs of electrodes sometimes showed highly correlated activity without similar high levels in intervening electrodes. Each pair of electrodes showed high variability at corresponding time intervals across trials. Averaging nearest-neighbor correla-

tion coefficients across trials revealed no pre- or post-stimulus time interval with differentially large correlation. No consistently high correlations were found at time segments corresponding to labeled peaks of the average evoked potentials.

In order to draw statistical inferences on the degree and extent of spatio-temporal correlations, bootstrap methods (Gevins et al., 1989; Cressie, 1993; Efron and Tibshirani, 1993) were devised. These methods use the data themselves to compute probability distributions for the variable that is estimated. An advantage of these methods is that they compensate for systematic biases in the data. In the variant used in the present study, ECoG time series as well as filtered random time series were used to derive expected probability distributions for the level of background and random fluctuations, respectively, in the correlations. Peak gamma band correlations of ± 0.8 or more were frequently observed between nearest- and next-to-nearest neighbor electrodes (separations of 1 cm and 1.4 cm). Intermittent peaks in correlation of this magnitude were also observed, although more infrequently, over separations greater than 1.4 cm. The skewness of the correlation distributions was about -0.6 at 1 cm but decreased to background levels at distances of 2 cm or more. The distributions were generally independent of the locations of the electrodes in the somatosensory, motor and pre-motor cortices as long as the electrodes were within the same gyrus. Across sulci, the distributions reduced to background levels at (surface) separations of 1.4 cm or more. Distributions beyond spatial scales of 2 cm were generally not statistically different ($P > 0.01$) and were therefore referred as background distributions. The background distribution itself differed from the noise distribution ($P < 0.005$). This difference is suggestive of systematic relations in short duration temporal correlations inherent in the ECoG, but not present in the noise, perhaps attributable to the shared time constants and feedback delays of the diverse neural populations that generate the synaptic currents underlying the ECoGs (Freeman, 1992).

The minimum duration of segments of high correlation was determined from the first zero crossing of the auto-correlation function of 50–75 msec (similar figures have been reported elsewhere, see, for example, Graf and Elbert, 1990). The maximal window length over which signals from electrodes separated by 1 cm were highly correlated was examined by computing the number of peaks as a function of the window size. The number of peaks decreased to noise levels for window lengths of about 300–375 msec and background levels at window lengths of about 175–250 msec. Based on these bounds, the mean correlation duration – the time interval over which the ECoG at distances of 1 cm was spatially correlated – was estimated to be about 150 msec which is in the theta-alpha band range of the ECoG. This estimate is in agreement with durations of gamma bursts reported in the olfactory system, visual cortex and somatosensory cortex. For win-

dows 150 msec in duration, the rate of occurrence of significant peaks in the correlations was about 1.3/sec. This figure is considerably higher than the (liberal) estimates of expected noise and background values, 0.39/sec and 0.45/sec respectively, obtained with 100 msec windows.

The findings suggest that domains of locally correlated gamma band ECoG activity are limited to less than 2 cm on the human cortical surface. The WHM of stimulus evoked potential peaks was also less than 2 cm in both patients. Spectral modulation by stimulus and response in the gamma band was detected across somewhat greater distances (3–5 cm) and in the mu band across 4–6 cm. These findings are consistent with the finding of a superficial source for high frequency bursts in primate sensorimotor cortex at depths of 0.8 mm (Mitzdorf, 1991; Murthy and Fetz, 1992) and suggest the presence of neuronal mechanisms to delimit the extent of domains of spatial correlations in human gamma band ECoG.

The excess in the number of high correlations above the number found for noise cannot be explained by volume conduction, owing to the large number of instances of drastically different correlation values in 3-way pairs, and to their rapid changes with time. Rather, they may perhaps be manifestations of the type of spatial correlations found with finer spatial grids over smaller spatial windows in animals. In the human neocortex, a further complication arises from complex contributions to the surface potential due to sulci (Mitzdorf, 1991), which can have depths of up to 35 mm (Talairach and Tournoux, 1988). The relative contribution of these factors is a topic for future studies.

These findings suggest that in human neocortex, identifiable spatial patterns based on local commonality of gamma band wave form, such as those found in animal paleocortex (Freeman and Baird, 1987) and neocortex (Freeman and Barrie, 1994), may exist only on spatial scales below 2 cm. Although evoked potential measurements of widespread cortical networks activated in sensory, motor and cognitive tasks are well established (Gevins et al., 1981, 1983, 1987, 1994; ; Hillyard and Picton, 1987; Picton, 1988; Regan, 1989; Gevins and Cuttillo, 1993), signs of such interactions in the gamma band were not revealed in the present study. While the nature of gamma band spatial events and their behavioral correlates is well defined in studies across 5 mm × 5 mm arrays in animal paleocortex and neocortex, the nature of spatio-temporal events and their correlates across larger scales is still unknown.

Acknowledgements

This research was supported by Grant NIMH-MH43324 to EEG Systems Lab.

References

- Arroyo, S., Lesser, R.P. and Gordon, B. (1993) Functional significance of the mu rhythm of human cortex: an electrophysiologic study with subdural electrodes. *Electroenceph. clin. Neurophysiol.*, 87: 76–87.
- Bressler, S.L., Coppola, R. and Nakamura, R. (1993) Episodic multiregional cortical coherence at multiple frequencies during visual task performance. *Nature*, 366: 153–156.
- Bullock, T.H., Achimowicz, J.Z. and McClune, M.C. (1992) Coherence in human subdural EEG has fine structure in space and time. *Soc. Neurosci. Abst.*, 2: 906.
- Calvin, W.H. (1994) The emergence of intelligence. *Scient. Am.*, 271: 100–107.
- Cressie, N.A.C. (1993) *Statistics for Spatial Data*. Wiley, New York.
- Eckhorn, R., Bauer, R., Jordan, W., Brosch, M., Munk, M. and Reitboeck, H.J. (1988) Coherent oscillations: a mechanism of feature linking in the visual cortex? *Biol. Cybernet.*, 60: 121–130.
- Efron, B. and Tibshirani, R.J. (1993) *An Introduction to the Bootstrap*. Chapman and Hall, New York.
- Freeman, W.J. (1987) In search of the physiological basis of the EEG. In: A.S. Gevins and A. Rémond (Eds.), *Handbook of EEG and Clinical Neurophysiology (Revised Ser.)*, Vol. 1. Elsevier, Amsterdam, pp. 583–664.
- Freeman, W.J. (1991) The physiology of perception. *Scient. Am.*, 264: 78–85.
- Freeman, W.J. (1992) Tutorial in neurobiology: from single neurons to brain chaos. *Int. J. Bifurc. Chaos*, 2: 451–482.
- Freeman, W.J. and Baird, B. (1987) Relation of olfactory EEG to behavior: spatial analysis. *Behav. Neurosci.*, 3: 393–408.
- Freeman, W.J. and Barrie, J.M. (1993) Spatio-temporal patterns of visual, auditory, and somesthetic EEGs in perception by trained rabbits. *Soc. Neurosci. Abst.*, 1.
- Freeman, W.J. and Barrie, J.M. (1994) Chaotic oscillations and the genesis of meaning in cerebral cortex. In: G. Buzsáki (Ed.), *Temporal Coding in the Brain*. Springer, Berlin.
- Freeman, W.J. and Grajski, K.A. (1987) Relation of olfactory EEG to behavior: factor analysis. *Behav. Neurosci.*, 101: 766–777.
- Freeman, W.J. and Van Dijk, B.W. (1987) Spatial patterns of visual cortical fast EEG during condition reflex in a rhesus monkey. *Behav. Brain Sci.*, 422: 267–276.
- Freeman, W.J. and Viana di Prisco, G. (1986) Relation of olfactory EEG on behavior: time series analysis. *Behav. Neurosci.*, 100: 753–763.
- Gevins, A. (1980) Pattern recognition of brain electrical potentials. *IEEE Trans. Patt. Anal. Mach. Intell.*, PAMI-2, 5: 383–404.
- Gevins, A. and Cuttillo, B.A. (1993) Spatiotemporal dynamics of component processes in human working memory. *Electroenceph. clin. Neurophysiol.*, 87: 128–143.
- Gevins, A., Zeitlin, G.M., Yingling, C.D., Doyle, J.C., Dedon, M.F., Schaffer, R.E., Roumasset, J.T. and Yeager, C.L. (1979) EEG patterns during cognitive tasks. I. Methodology and analysis of complex behaviors. *Electroenceph. clin. Neurophysiol.*, 47: 693–703.
- Gevins, A., Doyle, J.C., Cuttillo, B.A., Schaffer, R.E., Tannehill, R.L., Ghannam, J.H., Gilcrease, V.A. and Yeager, C.L. (1981) Electrical potentials in human brain during cognition: new method reveals dynamics patterns of correlation. *Science*, 213: 918–922.
- Gevins, A., Schaffer, R.E., Doyle, J.C., Cuttillo, B.A., Tannehill, R.L. and Bressler, S.L. (1983) Human neuroelectric patterns predict performance accuracy. *Science*, 220: 97–99.
- Gevins, A., Morgan, N.H., Bressler, S.L., Cuttillo, B.A., White, R.M., Illes, J., Greer, D., Doyle, J.C. and Zeitlin, G.M. (1987) Shadows of thought: shifting lateralization of human brain patterns during brief visuomotor task. *Science*, 235: 580–585.
- Gevins, A., Bressler, S.L., Morgan, N.H., Cuttillo, B.A., White, R.M., Greer, D. and Illes, J. (1989) Event-related covariances during a

- bimanual visuomotor task. I. Methods and analysis of stimulus- and response-locked data. *Electroenceph. clin. Neurophysiol.*, 74: 58–75.
- Gevins, A.S., Cutillo, B.A., Desmond, J.E., Ward, M., Bressler, S.L. and Laxer, K. (1994) Subdural grid recordings of distributed neocortical networks with somatosensory discrimination. *Electroenceph. clin. Neurophysiol.*, 92: 282–290.
- Gevins, A., Menon, V., Desmond, J.E., Smith, M.E., Le, J. and Martin, N.K. (1996) High resolution EEG. II. Application to late component transient evoked potentials recorded during a somatosensory discrimination task. Submitted.
- Graf, K.E. and Elbert, T. (1990) Dimensional analysis of the waking EEG. In: E. Başar (Ed.), *Chaos in Brain Function*. Springer, New York.
- Gray, C.M., Engel, A.K. and Singer, W. (1989) Oscillatory responses in cat visual cortex exhibit inter-columnar synchronization which reflects global stimulus properties. *Nature*, 338: 334–337.
- Hardcastle, V.G. (1994) Psychology's binding problem and possible neurobiological solutions. *J. Consc. Stud.*, 1: 66–90.
- Hays, W. (1994) *Statistics*, 5th Edn. Saunders, Philadelphia, PA.
- Hillyard, S.A. and Picton, T. (1987) Electrophysiology of cognition. In: F. Plum (Ed.), *Handbook of Physiology: Higher Functions of the Nervous System*, Sect. 1. Vol. V. Higher Functions of the Brain, Part 2. American Physiological Society, Bethesda, MD, pp. 519–584.
- Llinás, R. and Ribary, U. (1993) Coherent 40-Hz oscillations characterize dream state in humans. *Proc. Nat. Acad. Sci. (USA)*, 90: 2078–2081.
- Menon, V., Freeman, W.J. and Gevins, A.S. (1994) Spatio-temporal correlations in human gamma band electrocorticograms. *Soc. Neurosci. Abst.*, 20: 1003.
- Mitzdorf, U. (1991) Physiological sources of evoked potentials. In: C.H.M. Brunia, G. Mulder and M.N. Verbaten (Eds.), *Event-Related Brain Research*. *Electroenceph. clin. Neurophysiol.*, Suppl. 42. Elsevier, Amsterdam, pp. 47–57.
- Murthy, V.N. and Fetz, E.E. (1992) Coherent 25- to 35-Hz oscillations in the sensorimotor cortex of awake behaving monkeys. *Proc. Nat. Acad. Sci. (USA)*, 89: 5670–5674.
- Pfurtscheller, G. and Neuper, C. (1988) Simultaneous EEG 10 Hz desynchronization and 40 Hz synchronization during finger movements. *NeuroReport*, 3: 1057–1060.
- Picton, T.W. (1988) Human Event-Related Potentials. *Handbook of Electroencephalography and Clinical Neurophysiology (Revised Ser.)*, Vol. 3. Elsevier, Amsterdam.
- Press, W.H., Teukolsky, S. and Vetterling, W. (1992) *Numerical Recipes in C: the Art of Scientific Programming*. Cambridge University Press, Cambridge.
- Regan, D. (1989) *Human Brain Electrophysiology*. Elsevier, New York.
- Sanes, J.N. and Donoghue, J.P. (1993) Oscillations in local field potentials of the primate motor cortex during voluntary movement. *Proc. Nat. Acad. Sci. (USA)*, 90: 4470–4474.
- Talairach, J. and Tournoux, P. (1988) *Co-planar Stereoscopic Atlas of the Human Brain*. Thieme, Stuttgart.
- Viana di Prisco, G. and Freeman, W.J. (1985) Odor-related bulbar EEG spatial pattern analysis during appetitive conditioning in rabbits. *Behav. Neurosci.*, 99: 962–978.